Molecular Refrigeration

DOI: 10.1002/ange.201308240

Fluoride-Bridged $\{Gd^{III}_3M^{III}_2\}$ (M = Cr, Fe, Ga) Molecular Magnetic Refrigerants**

Kasper S. Pedersen, Giulia Lorusso, Juan José Morales, Thomas Weyhermüller, Stergios Piligkos, Saurabh Kumar Singh, Dennis Larsen, Magnus Schau-Magnussen, Gopalan Rajaraman, Marco Evangelisti, and Jesper Bendix**

Abstract: *The reaction of fac-$[M^{III}F_3(Me_3tacn)]\cdot x\,H_2O$ with $Gd(NO_3)_3\cdot 5H_2O$ affords a series of fluoride-bridged, trigonal bipyramidal $\{Gd^{III}_3M^{III}_2\}$ (M = Cr (**1**), Fe (**2**), Ga (**3**)) complexes without signs of concomitant GdF_3 formation, thereby demonstrating the applicability even of labile fluoride-complexes as precursors for 3d–4f systems. Molecular geometry enforces weak exchange interactions, which is rationalized computationally. This, in conjunction with a lightweight ligand sphere, gives rise to large magnetic entropy changes of 38.3 $J\,kg^{-1}\,K^{-1}$ (**1**) and 33.1 $J\,kg^{-1}\,K^{-1}$ (**2**) for the field change 7 T→0 T. Interestingly, the entropy change, and the magneto-caloric effect, are smaller in **2** than in **1** despite the larger spin ground state of the former secured by intramolecular Fe–Gd ferromagnetic interactions. This observation underlines the necessity of controlling not only the ground state but also close-lying excited states for successful design of molecular refrigerants.*

Paramagnetic molecules with large spin and negligible magnetic anisotropy have received immense interest in the last few years owing to the demonstration of large magneto-caloric effects (MCE).[1] The effect is inherently related to the magnetic entropy increase at low temperatures, which follows an adiabatic demagnetization. Particularly, it is of interest to link the magnetic centers, and shield them magnetically from adjacent molecules, by lightweight ligands to furnish a high magnetic density, which ultimately favors a large MCE.[1c] For an exchange-coupled polynuclear complex, if only the ground-spin manifold S_T is considered, the magnetic entropy is given by $S_m = R\ln(2S_T+1)$. The type and strength of the magnetic interactions determine the way in which the entropy is gradually released with decreasing temperature, which occurs more abruptly in the temperature range where the interactions are important.[1a,2] Ultimately, on increasing the field change ΔB, the change of entropy $-\Delta S_m$ reaches its maximum value, corresponding to the full entropy content of the system, namely, the entropy sum over all single-ion spins S_i, that is, $R\Sigma_i \ln(2S_i+1)$. It thus seems promising to combine Gd^{III} ($S_{Gd} = 7/2$) with "magnetically isotropic" transition-metal ions, such as Cr^{III} ($S_{Cr} = 3/2$) or high-spin Fe^{III} ($S_{Fe} = 5/2$), preferably connected by weak intramolecular ferromagnetic interactions. Recently, Winpenny and co-workers,[3] and we,[4] reported the first examples of polynuclear complexes incorporating fluoride-bridged $\{Cr^{III}–F–Ln^{III}\}$ units. These systems owe their existence to the robust character of Cr^{III} (d^3) complexes by avoiding precipitation of insoluble LnF_3.[5] Unfortunately, this fact imposes strong limitations on the chemistry that can be exploited, and we herein demonstrate that fluoride-bridged 3d–4f polynuclear complexes can indeed also be prepared from labile transition metal fluoride complexes.

As we recently reported, the reaction of *fac*-$[CrF_3(Me_3tacn)]\cdot 4H_2O$ (Me_3tacn = *N*,*N*′,*N*″-trimethyl-1,4,7-triazacyclononane) with $Nd(NO_3)_3\cdot 6H_2O$ yields a fluoride-bridged $\{Nd_3Cr_2\}$ trigonal bipyramid (TBP).[4b] Performing the same reaction employing $Gd(NO_3)_3\cdot 5H_2O$ affords the closely related $[\{CrF_3(Me_3tacn)\}_2Gd_3F_2(NO_3)_7(H_2O)(CH_3CN)]\cdot 4CH_3CN$ (**1**), which can be considered as a lightweight analogue of the $[\{CrF_3(Me_3tame)\}_2Gd_3F_3(hfac)_6]\cdot 7CH_3CN$ TBP-shaped pentanuclear system that exhibits good cooling properties (Me_3tame = 1,1,1-tris{(methylamino)methyl}ethane, hfacH = 1,1,1,5,5,5-hexafluoroacetylacetone). Although this result is unsurprising, the analogous reaction with novel *fac*-$[FeF_3(Me_3tacn)]\cdot H_2O$ and *fac*-$[GaF_3(Me_3tacn)]\cdot 4H_2O$, conveniently synthesized from FeF_3 and $GaF_3\cdot 3H_2O$, respectively, yields isostructural $[\{MF_3(Me_3tacn)\}_2Gd_3F_2(NO_3)_7(H_2O)(CH_3CN)]\cdot 4CH_3CN$ (M = Fe (**2**), Ga (**3**); Figure 1) without any signs of GdF_3 formation. Notably, the presence of any hydroxide bridging can be safely ruled out based on electrospray mass spectra (Supporting Information, Figures S4–S6).

[*] K. S. Pedersen, Dr. S. Piligkos, D. Larsen, M. Schau-Magnussen, Prof. Dr. J. Bendix
Department of Chemistry, University of Copenhagen
Universitetsparken 5, 2100 Copenhagen (Denmark)
E-mail: bendix@kiku.dk

Dr. G. Lorusso, J. J. Morales, Dr. M. Evangelisti
Instituto de Ciencia de Materiales de Aragón, Departamento de Física de la Materia Condensada, CSIC-Universidad de Zaragoza
50009 Zaragoza (Spain)
E-mail: evange@unizar.es

Dr. T. Weyhermüller
Max Planck Institute for Chemical Energy Conversion
Mülheim an der Ruhr (Germany)

S. K. Singh, Dr. G. Rajaraman
Department of Chemistry, Indian Institute of Technology Bombay
Powai, Mumbai (India)

[**] K.S.P. and S.P. thank the Danish Ministry of Science Innovation and Higher Education for an EliteForsk travel grant and a Sapere Aude Fellowship (10-081659), respectively. G.L., J.J.M., and M.E. acknowledge financial support by the Spanish MINECO through grant MAT2012-38318-C03-01. G.L. is also grateful to the EC for a Marie Curie-IEF (PIEF-GA-2011-299356). G.R. would like to thank DST, India (SR/S1/IC-41/2010; SR/NM/NS-1119/2011) for funding and IITB for HPC resources. S.K.S. thanks CSIR for a SRF fellowship.

Supporting information for this article is available on the WWW under http://dx.doi.org/10.1002/anie.201308240.

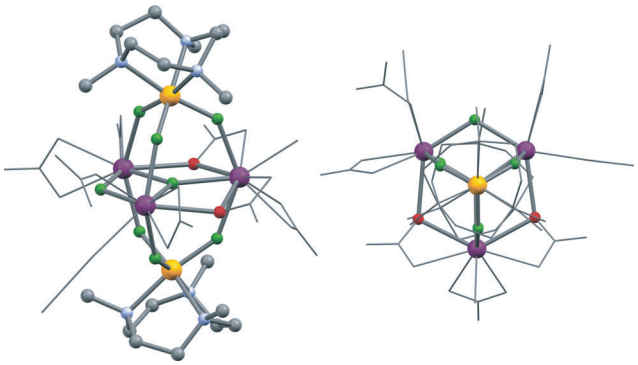

Figure 1. The structure of **2** shown in perspective (left) and along the Fe···Fe direction (right). Gd purple, Fe yellow, F green, O red, N blue, C gray. For clarity, the auxiliary Gd ligand sphere is shown as a wire-frame.

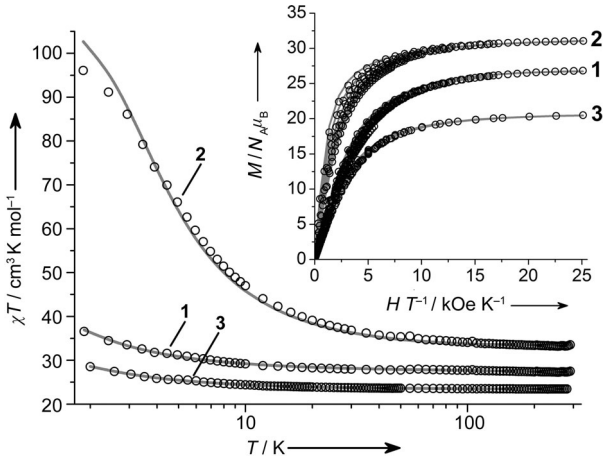

Figure 2. Temperature dependence of the χT product ($\chi = M/H$, $H = 1000$ Oe) of **1**–**3**. The solid gray lines are best fits as described in the text. Inset: Reduced magnetization and best fits for **1**–**3** at selected low temperatures.

The capping *fac*-$[FeF_3(Me_3tacn)]$ units (angle Gd-F-Fe = 137.1(1)°–143.1(1)°) impose an approximately isosceles $\{Gd_3\}$ triangle. Two edges consist of $\eta^1{:}\eta^2{:}\mu_2$-bridging nitrate ions and one edge consists of a μ_2-fluoride (Figure 1). Additionally, the center furnishes a single μ_3-fluoride bridge close to the $\{Gd_3\}$ plane with Gd-(μ_3-F)-Gd angles of 110.43(11)°, 124.64(12)°, and 124.93(11)°. Compounds **2** and **3** add to the tiny family of fourth row/transition element–lanthanide, fluoride-bridged systems, which, in addition to the Cr^{III} systems,[3,4] only encompasses $[La\{(C_5Me_4Et)_2Ti_2F_7\}_3]$ and $[Ln\{(C_5Me_5)_2Ti_2F_7\}_3]$ (Ln = Pr, Nd).[6] These latter systems, however, rely on the pronounced "hard" metal ions Ti^{IV} and Ln^{III}, which compete efficiently for fluoride abstraction. Neither Fe^{III} nor Ga^{III} are as hard as Ti^{IV} or kinetically robust as Cr^{III}, but, surprisingly, exhibit similar reactivity towards Gd^{III}. The lightweight structures and the larger spin possessed by high-spin Fe^{III} over Cr^{III} fuelled our curiosity whether improved molecular refrigerants could result. The magnetic data for the isolated *fac*-$[CrF_3(Me_3tacn)]\cdot 4H_2O$ and *fac*-$[FeF_3(Me_3tacn)]\cdot H_2O$ complexes are shown in the Supporting Information (Figures S7, S8). As expected, the magnetic data are largely reminiscent of a Curie behavior with temperature-independent χT products approaching the values expected for $S_{Cr} = 3/2$ and $S_{Fe} = 5/2$, with a *g*-factor of $g \approx 2$. The temperature dependence of the magnetic susceptibility for **1**, **2**, and **3** is shown in Figure 2 in the form of χT products. The field dependencies of the magnetizations are given in Figure 2 (inset) and in the Supporting Information, Figures S9–S11. The high-temperature values of the χT products (**1** 27.3 $cm^3 mol^{-1} K^{-1}$, **2** 33.3 $cm^3 mol^{-1} K^{-1}$, and **3** 23.6 $cm^3 mol^{-1} K^{-1}$) are in good agreement with the values expected for the spin-only contributions from the uncorrelated ions. On cooling, all χT products increase to reach 36.6, 96.1, and 28.5 $cm^3 mol^{-1} K^{-1}$ for **1**, **2**, and **3**, respectively. This behavior suggests the presence of intra-complex ferromagnetic interactions for all of the compounds. The magnetic data were fitted by use of the Levenberg–Marquardt algorithm[7] and by numerical diagonalization of the matrix representation of the isotropic spin-Hamiltonian (1):

$$\hat{H} = g\mu_B \mathbf{B} \cdot \sum_i \hat{\mathbf{S}}_i + J_{ij} \sum_{i,j>i} \hat{\mathbf{S}}_i \cdot \hat{\mathbf{S}}_j \qquad (1)$$

where the indices *i* and *j* run through the constitutive single ions of each compound, *g* is the single-ion *g*-factor, fixed to 2.0 for all ions, $\hat{\mathbf{S}}$ is a spin operator, and J_{ij} is the isotropic exchange coupling parameter between the *i*th and *j*th centers. For **1** and **2**, the χT product and the low-temperature variable-field magnetization (M vs. H) data can be fitted using just two parameters, namely $J_{M\text{-}Gd}$ and $J_{Gd\text{-}Gd}$, while fitting the χT data against spin-Hamiltonian (1) results in strongly correlated parameters. The modeling of the magnetic data of **3** affords a good estimation of the Gd–Gd exchange interaction void of complicating, additional interactions. Simultaneous fitting of the χT product and the M vs. H data yields $J_{Gd\text{-}Gd} = -0.028\ cm^{-1}$. The best-fit curves are shown as solid lines in Figure 2 and in the Supporting Information. The data of **1** and **2** were fitted with only $J_{M\text{-}Gd}$ as the free parameter assuming transferability of $J_{Gd\text{-}Gd}$ from **3** to **1** and **2**. For **1**, this yielded $J_{Cr\text{-}Gd} = -0.046\ cm^{-1}$ and $-0.036\ cm^{-1}$, as obtained from the χT product and magnetization data, respectively. Analogously, for **2**, the best-fit $J_{Fe\text{-}Gd}$ parameter values were $-0.25\ cm^{-1}$ (from χT) and $-0.26\ cm^{-1}$ (from M vs. H).

In previous studies,[8] we have established a magneto-structural correlation of the $J_{Cr\text{-}Gd}$ parameter as function of the Cr-F-Gd bridging angle. The average Cr-F-Gd bridging angle of 141.5° in **1**, should according to this correlation result in a very small positive $J_{Cr\text{-}Gd}$ value. This is in reasonable agreement with the vanishing best-fit $J_{Cr\text{-}Gd}$ parameter value. To gain insight in the magnitude and sign of the Fe^{III}–F–Gd^{III} interaction, DFT calculations employing the experimental geometry were undertaken. The resulting parameter values are $J_{Fe\text{-}Gd} = -0.35\ cm^{-1}$ and $J_{Gd\text{-}Gd} = -0.02\ cm^{-1}$, which are also in good agreement with the experimental findings and previous theoretical studies.[9]

Furthermore, we performed calculations on the dinuclear model $[Fe^{III}F_2(py)_4Gd^{III}(hfac)_4]$ (py = pyridine) to develop a magneto-structural model for the Fe^{III}–F–Gd^{III} unit mimicking our approach for the Cr^{III} analogue.[8] This simple approach is justified by the equality of the average Fe–F (1.91 Å) and Cr–F (1.91 Å) bonds in **1** and **2**. DFT calcu-

lations yield a ferromagnetic coupling ($J = -1.1$ cm^{-1}) for the dinuclear model, in contrast to the Cr^{III} analogue where an antiferromagnetic coupling was calculated. As discussed by Ruiz and co-workers, the interaction of the 3d orbitals of transition metals with the 5d orbitals of Gd^{III} plays a key role in controlling the sign of the magnetic interaction.[10] Previously, we established the mechanism of magnetic coupling for generic 3d Gd^{III} pairs where the crucial role of empty 5d orbitals of Gd^{III} was illustrated.[11] Specifically, the occupation of 5d orbitals is linked to the sign of the coupling constant, with larger occupation leading to more ferromagnetic interaction, in structurally related compounds.[11b] For Cr^{III}, with $(t_{2g})^3$ configuration, interaction with Gd^{III} 5d orbitals is relatively smaller as compared to Fe^{III} where the e_g orbitals promote stronger delocalization and interaction with the Gd^{III} 5d orbitals. The differential occupancy is evident also from the NBO calculations (see the Supporting Information for details). The overlap between 3d and 4f orbitals, which generally contributes to antiferromagnetic coupling, is also detected to be significantly less for the Fe^{III}–Gd^{III} pair compared to Cr^{III}–Gd^{III} analogues (Supporting Information, Table S3). The angular dependence of $J_{Fe\text{-}Gd}$ in {Fe^{III}-F-Gd^{III}} (Figure 3) shows the magnitude of the ferromagnetic $J_{Fe\text{-}Gd}$ to increase with the bridging angle, while for {Cr^{III}–F–Gd^{III}} an opposite trend was established.[8] As the angle increases, the interaction of the Fe^{III} d_{z^2} orbital with Gd^{III} 5d orbitals is expected to be large, leading to stronger ferromagnetic coupling for the Fe^{III}–Gd^{III} pair. For the Cr^{III}–Gd^{III} pair at larger angles, the spin-bearing orbitals of Cr^{III} and the Gd^{III} d-orbitals become orthogonal, leading to a decrease in the interaction and less (more) ferromagnetic (antiferromagnetic) coupling. The spin density analysis (Figure 3) reflects the points discussed where Cr^{III} has gained spin density while there is significant reduction on the Fe^{III} (3.09 vs. 4.28 for Cr^{III} and Fe^{III}, respectively). This suggests a spin-polarization mechanism for the Cr^{III}–Gd^{III} unit and both spin-polarization and a delocalization mechanism operational for Fe^{III}–Gd^{III}. This is visually directly observable in the significant departure from spherical shape of the spin-density distribution around Fe^{III}.

The different magnitude of $J_{Cr\text{-}Gd}$ and $J_{Fe\text{-}Gd}$ is also observed in the experimental specific heat of **1** and **2**, respectively (Supporting Information, Figure S12) together with the calculated Schottky anomalies for the paramagnetic ions at the corresponding fields (solid lines). Indeed, while for **1** the intramolecular magnetic interactions are already decoupled for fields larger than 1 T, for **2**, fields larger than 7 T are necessary. A prominent feature in **2** is the kink at $T_c = 0.65$ K that we ascribe to a magnetic phase transition that is driven by dipolar interactions. We notice that the magnetic entropy at T_c amounts to about 3.2 k_B per molecular spin (Supporting Information, Figure S12), which is close to the value corresponding to the highest possible spin per molecule obtained in case of ferromagnetic alignment, that is, $k_B \ln(2S_T+1) = 3.47\ k_B$, where $S_T = 3S_{Gd} + 2S_{Fe} = 31/2$. Thus, we conjecture that the phase transition takes place concomitantly with the establishment of intramolecular alignment of spins. Indeed, T_c is of the same order as the dipolar interaction energy between nearest-neighbor $S_T = 31/2$ molecules, that is, $\mu^2/r^3 \approx 0.3$ K, where $r \approx 12$ Å is the intermolecular distance. In contrast, $J_{Cr\text{-}Gd}$ in **1** is not sufficiently strong to compete with thermal fluctuations. Thus, neither an intramolecular ordering nor a phase transition is observed for **1**.

The MCE is evaluated by obtaining the isothermal magnetic entropy changes $-\Delta S_m$ from the entropy data. We also use the magnetization data (Supporting Information, Figures S9–S11) for the same purpose by means of the Maxwell relation $\Delta S_m(T) = \int[\partial M(T,B)/\partial T]_B\ dB$. From Figure 4, the maximum $-\Delta S_m$ values for the largest ΔB (from 7 T to 0 T) are 38.3 J kg^{-1}K^{-1} ($T = 2.0$ K) and 33.1 J kg^{-1}K^{-1} ($T = 4.2$ K) for **1** and **2**, respectively. The maximum entropy value involved, corresponding to $3S_{Gd}$ and $2S_{Cr}$ (S_{Fe}), is calculated as 43.4 (47.1) J kg^{-1}K^{-1} for **1** (**2**). Therefore, for ΔB larger than the field needed to fully overwhelm the cumulative effect of magnetic interactions

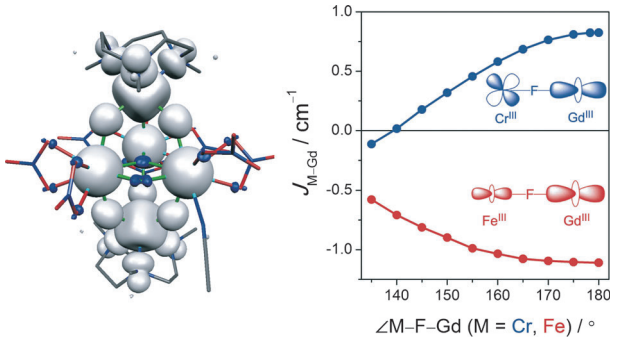

Figure 3. DFT-computed spin densities (left) for complex **2** drawn with isosurface value of 0.003 a_0^{-3} (a_0 = Bohr length) and DFT-based magneto-structural correlations (right) developed for the model complex described in the text.

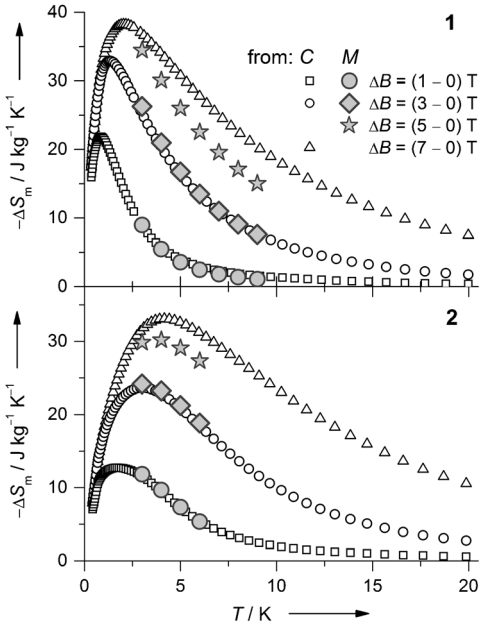

Figure 4. Magnetic entropy changes $-\Delta S_m$ corresponding to the labeled magnetic field changes, ΔB, for **1** (top) and **2** (bottom), as obtained from specific heat C and magnetization M data. See the Supporting Information, Figure S15 for a zoom of the low-temperature region.

involved, a larger $-\Delta S_m$ should occur in **2** rather than **1**. Otherwise, a larger $-\Delta S_m$ would be expected in the case of weaker magnetic correlations, as experimentally observed for $\Delta B \leq 7$ T. Indeed, a weaker coupling promotes a relatively larger number of low-lying excited spin states, thus favoring a larger field-dependence of the MCE. Finally, we point out that the experimental $-\Delta S_m$ of **1** is extremely large for a 3d–4f complex and comparable to the best magnetic molecular refrigerants at liquid-helium temperatures.[12]

In summary, a small family of unusual fourth-row metal-ion–lanthanide complexes with bridging fluoride ions is reported. The combination of lightweight auxiliary ligands and tunable interaction by choice of metal ion makes these systems interesting modules for low-temperature cooling applications.

Received: September 19, 2013
Published online: February 6, 2014

Keywords: density functional calculations · fluoride ligands · lanthanides · magnetic properties · magnetic refrigeration

[1] a) M. Evangelisti, E. K. Brechin, *Dalton Trans.* **2010**, *39*, 4672; b) J. W. Sharples, D. Collison, *Polyhedron* **2013**, *54*, 91; c) M. Evangelisti in *Molecular Magnets*, *NanoScience and Technology* (Eds.: J. Bartolomé, F. Luis, J. F. Fernández), Springer, Berlin, pp. 365–387, **2014**.

[2] M. Evangelisti, A. Candini, M. Affronte, E. Pasca, L. J. de Jongh, R. T. W. Scott, E. K. Brechin, *Phys. Rev. B* **2009**, *79*, 104414.

[3] A. McRobbie, A. R. Sarwar, S. Yeninas, H. Nowell, M. L. Baker, D. Allan, M. Luban, C. A. Muryn, R. G. Pritchard, R. Prozorov, G. Timco, F. Tuna, G. F. S. Whitehead, R. E. P. Winpenny, *Chem. Commun.* **2011**, *47*, 6251.

[4] a) J. Dreiser, K. S. Pedersen, C. Piamonteze, S. Rusponi, Z. Salman, M. E. Ali, M. Schau-Magnussen, C. A. Thuesen, S. Piligkos, H. Weihe, H. Mutka, O. Waldmann, P. Oppeneer, J. Bendix, F. Nolting, H. Brune, *Chem. Sci.* **2012**, *3*, 1024; b) T. Birk, K. S. Pedersen, C. A. Thuesen, T. Weyhermüller, M. Schau-Magnussen, S. Piligkos, H. Weihe, S. Mossin, M. Evangelisti, J. Bendix, *Inorg. Chem.* **2012**, *51*, 5435; c) C. A. Thuesen, K. S. Pedersen, M. Schau-Magnussen, M. Evangelisti, J. Vibenholt, S. Piligkos, H. Weihe, J. Bendix, *Dalton Trans.* **2012**, *41*, 11284.

[5] J. Dreiser, K. S. Pedersen, T. Birk, M. Schau-Magnussen, C. Piamonteze, S. Rusponi, T. Weyhermüller, H. Brune, F. Nolting, J. Bendix, *J. Phys. Chem. A* **2012**, *116*, 7842.

[6] a) F. Perdih, A. Demsar, A. Pevec, S. Petricek, I. Leban, G. Giester, J. Sieler, H. W. Roesky, *Polyhedron* **2001**, *20*, 1967; b) A. Pevec, M. Mrak, A. Demsar, S. Petricek, H. W. Roesky, *Polyhedron* **2003**, *22*, 575.

[7] W. H. Press, S. A. Teukolsky, W. T. Vetterling, B. P. Flannery, *Numerical Recipes in C*: *The Art of Scientific Computing*, *2nd ed.*, Cambridge University Press, Cambridge, **1992**.

[8] S. K. Singh, K. S. Pedersen, M. Sigrist, C. A. Thuesen, M. Schau-Magnussen, S. Piligkos, H. Mutka, H. Weihe, G. Rajaraman, J. Bendix, *Chem. Commun.* **2013**, *49*, 5583.

[9] T. Rajeshkumar, S. K. Singh, G. Rajaraman, *Polyhedron* **2013**, *52*, 1299.

[10] E. Cremades, S. Gómez-Coca, D. Aravena, S. Alvarez, E. Ruiz, *J. Am. Chem. Soc.* **2012**, *134*, 10532.

[11] a) S. K. Singh, N. K. Tibrewal, G. Rajaraman, *Dalton Trans.* **2011**, *40*, 10897; b) S. K. Singh, G. Rajaraman, *Dalton Trans.* **2013**, *42*, 3623; c) G. Rajaraman, F. Totti, A. Bencini, A. Caneschi, R. Sessoli, D. Gatteschi, *Dalton Trans.* **2009**, 3153; d) J. Paulovic, F. Cimpoesu, M. Ferbinteanu, K. Hirao, *J. Am. Chem. Soc.* **2004**, *126*, 3321; e) T. Rajeshkumar, G. Rajaraman, *Chem. Commun.* **2012**, *48*, 7856; f) T. Rajeshkumar, S. K. Singh, G. Rajaraman, *Polyhedron* **2013**, *52*, 1299.

[12] a) M. Evangelisti, O. Roubeau, E. Palacios, A. Camón, T. N. Hooper, E. K. Brechin, J. J. Alonso, *Angew. Chem.* **2011**, *123*, 6736; *Angew. Chem. Int. Ed.* **2011**, *50*, 6606; b) Y.-Z. Zheng, E. M. Pineda, M. Helliwell, R. E. P. Winpenny, *Chem. Eur. J.* **2012**, *18*, 4161; c) Y.-Z. Zheng, M. Evangelisti, F. Tuna, R. E. P. Winpenny, *J. Am. Chem. Soc.* **2012**, *134*, 1057; d) S. Langley, N. Chilton, B. Moubaraki, T. Hooper, E. K. Brechin, M. Evangelisti, K. S. Murray, *Chem. Sci.* **2011**, *2*, 1166; e) J. W. Sharples, Y.-Z. Zheng, F. Tuna, E. J. L. McInnes, *Chem. Commun.* **2011**, *47*, 7650; f) J.-B. Peng, Q.-C. Zhang, X.-J. Kong, Y.-P. Ren, L.-S. Long, R.-B. Huang, L.-S. Zheng, Z. Zheng, *Angew. Chem.* **2011**, *123*, 10837; *Angew. Chem. Int. Ed.* **2011**, *50*, 10649; g) J.-B. Peng, Q.-C. Zhang, X.-J. Kong, Y.-Z. Zheng, Y.-P. Ren, L.-S. Long, R.-B. Huang, L.-S. Zheng, Z. Zheng, *J. Am. Chem. Soc.* **2012**, *134*, 3314; h) R. Sibille, T. Mazet, B. Malaman, M. François, *Chem. Eur. J.* **2012**, *18*, 12970; i) E. Colacio, J. Ruiz, G. Lorusso, E. K. Brechin, M. Evangelisti, *Chem. Commun.* **2013**, *49*, 3845; j) G. Lorusso, J. W. Sharples, E. Palacios, O. Roubeau, E. K. Brechin, R. Sessoli, A. Rossin, F. Tuna, E. J. L. McInnes, D. Collison, M. Evangelisti, *Adv. Mater.* **2013**, *25*, 4653.

